



Cite this: *Chem. Commun.*, 2016,
52, 13299

Received 3rd September 2016,
Accepted 19th October 2016

DOI: 10.1039/c6cc07215a

www.rsc.org/chemcomm

Improving O₂ reduction at an enzymatic biocathode: mimicking the lungs†

David P. Hickey, Krysti L. Knoche, Kelan Albertson, Carolina Castro, Ross D. Milton
and Shelley D. Minteer*

Here, we demonstrate the use of phospholipid micelles to enhance O₂ concentrations by two-fold at the surface of a bilirubin oxidase biocathode. Specifically, 1,2-diarachidoyl-sn-glycero-3-phosphocholine was used in a glucose enzymatic fuel cell to limit power losses due to O₂ transport, even in a quiescent solution.

Enzymatic fuel cells (EFCs) have rapidly developed as a possible power source for small implantable electronic devices. Utilizing an enzymatic catalyst at one or both the anode and cathode, EFCs are capable of operating under physiological pH and temperature. Advancements in enzymatic anode materials have provided dramatic improvements in bioanodic current density; however, comparatively little progress has been made towards biocathode development despite being commonly cited as limiting to the current output of EFCs.^{1–6} Unlike bioanodic substrates such as saccharides and short-chain alcohols that are highly water-soluble, biocathodic substrates are almost exclusively limited to reducible gases, such as molecular oxygen, that are only sparsely soluble in aqueous solutions.⁷ Organic solvents, such as hexane and perfluorodecalin, are highly effective at solubilizing O₂, but are incompatible with most biological systems.^{8,9} Hence, further biocathode development requires broadly applicable strategies for increasing O₂ concentration at the enzyme-modified electrode interface. Consequently, we considered utilizing lipid micelle solutions as a way to combine the high-oxygen solubility of organic solvents with the biocompatibility of aqueous solutions. Herein, we describe the ability of a phospholipid, phosphatidylcholine, to increase the apparent O₂ concentration at a bilirubin oxidase (BOx) biocathode, allowing for dramatically improved quiescent biocathodic current density.

Enzymatic biocathodes are generally constructed using a polymer to immobilize an O₂-reducing enzyme, such as laccase or bilirubin oxidase, onto the surface of a carbon electrode. During immobilization, the enzyme is either combined with a

redox mediator to act as an electron shuttle between the electrode and the enzyme's active site,^{10–12} or the enzyme is oriented toward the electrode surface to facilitate efficient direct electron transfer (DET).^{11,13–15} An extensive body of literature has demonstrated methods for enhancing electron transfer rates between O₂-reducing enzymes and electrode surfaces through either mediator-assisted electron transfer or DET; however, the maximum current densities (j_{\max}) for these systems can only be reached through a combination of rapid convection and O₂-bubbling throughout the electrochemical measurements. This highlights the need for techniques to improve O₂ transport, and indicates that further biocathode development requires that these challenges be met.

Calabrese Barton and co-workers predict that biocathodes should theoretically be able to achieve current densities of 60 mA cm^{−2}, wherein they list the primary obstacles to an ideal biocathode as enzyme surface coverage and O₂ transport.¹⁶ Even if enzyme surface coverage and electron transfer can be made ideal, the necessity of rapid convection and O₂-bubbling adds a substantial energy cost to fuel cell operation and limits the practical application of the resulting EFCs. Therefore, successful strategies for increasing O₂ solubility in a biocathode solution must specifically aim to increase the local transport of O₂ to the biocathode surface.

Artificial oxygen carriers (AOCs) have long been studied to address medical problems associated with hypoxia. The most widely studied AOCs for *in vivo* use include O₂-saturated hemoglobin derivatives and perfluorocarbon formulations; however, the application of these solutions in the context of EFCs is complicated by slow intermolecular O₂ transport and biological incompatibility as mentioned before.^{17,18} A possible alternative solution to the problem of aqueous O₂ solubility can be found in the human respiratory system, which uses phosphatidylcholine derivatives to enhance O₂ transport into the blood stream.¹⁹ Phospholipids make up the primary surfactant class found in the lungs to solubilize O₂ from the air into the blood stream. In this process, O₂ is solubilized into phospholipid surfactant bilayers upon expansion of lungs and subsequently absorbed

Departments of Chemistry and Materials Science and Engineering,
University of Utah, Salt Lake City, Utah 84112, USA. E-mail: minteer@chem.utah.edu
† Electronic supplementary information (ESI) available. See DOI: 10.1039/c6cc07215a



into alveolar cells where it is transferred into the blood stream. Pulmonary surfactants exist primarily in the solid phase, through which O_2 diffuses very slowly.²⁰ It is only the expansion of the lungs that creates the increased partial pressure necessary to force O_2 into the lipid bilayer. Based on this, we hypothesized that a solid phase phospholipid surfactant could be used to trap and store O_2 in an aqueous solution, thereby enhancing the effective concentration at a biocathode interface.

To initiate our investigation, we screened a range of commercially available phospholipids to determine their capacity to trap and store O_2 . This was accomplished amperometrically by bubbling O_2 through a phospholipid solution and, using a platinum rotating disk electrode (RDE) as an oxygen reduction catalyst, measuring the amount of time ($t_{1/2}$) required to reach 50% of j_{max} (detailed procedures and complete screening results provided in ESI† Table S1 and Fig. S2). An initial screen was performed on short chain phosphocholines such as 1,2-distearoyl-*sn*-glycero-3-phosphocholine (DSPC), 1- α -phosphatidylcholine (1- α -PC), 1,2-dioleoyl-*sn*-glycero-3-phosphoethanolamine (DOPE), 1,2-dipalmitoyl-*sn*-glycero-3-phosphothioethanol (DPTE) and 1,2-distearoyl-*sn*-glycero-3-phosphoethanolamine-*N*-[methoxy(PEG)₂₀₀₀] (DSPE-PEG₂₀₀₀). Solutions of 1- α -PC, DOPE, DPTE and DSPE-PEG₂₀₀₀ all exhibited $t_{1/2}$'s similar to solutions containing only buffer (400–500 s compared to 460 s in buffer). However, DSPC exhibited a residence time (880 ± 90 s) nearly double that of solutions containing buffer alone.

Based on our initial hypothesis, we suspected that the anomalously high retention time of DSPC would be coupled to its state of phase under the temperature being studied. To probe this supposition, we expanded our initial screen to include phosphocholines of varying chain length, and thus varying transition temperatures (Fig. 1). It should be noted that throughout the remainder of the manuscript, phosphocholines (PCs) of varying length will be referred to by their chain length for systematic simplicity (*i.e.* PC₁₂, PC₁₄, PC₁₆, PC₁₈ and PC₂₀ refer to DLPC, DMPC, DPPC, DSPC and DAPC, respectively). A comparison of $t_{1/2}$ with the corresponding transition temperature of

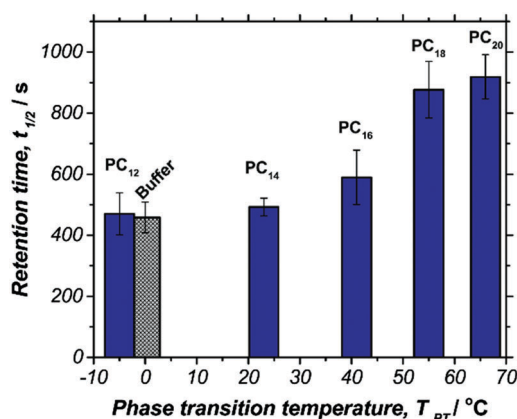


Fig. 1 PC phase transition temperature versus retention time ($t_{1/2}$) for solutions containing 0.5 mM PC. Retention time was measured amperometrically by platinum disk electrodes rotated at 500 rpm using 200 mM citrate/phosphate buffer at pH 6.5 and 25 °C.

the lipid reveals that PCs with a transition temperature above the experimental temperature exhibit significantly longer retention times; this supports the proposed correlation between state of phase and $t_{1/2}$. While RDE experiments were able to shed light on the nature of O_2 retention time for solutions of various phospholipids, the low catalytic activity of Pt under neutral pH and ambient temperature resulted in minimal variation in j_{max} .

With the primary goal of this work aimed at utilization in an EFC, we next sought to determine the impact of PCs on apparent O_2 concentration and retention time using a previously reported biocathode design based on bilirubin oxidase (BOx) with anthracene-modified carbon nanotubes on a 1 cm² Toray carbon paper electrode.²¹ Cyclic voltammetry (CV) was performed using BOx biocathodes suspended in O_2 -saturated buffers containing PCs of various chain length (Fig. 2). The resulting data indicates that the presence of PC with any length of chain increases j_{max} of the biocathode (ranging from $j_{max} = 0.73 \pm 0.20$ mA cm⁻² in PC₁₂ to $j_{max} = 1.14 \pm 0.15$ mA cm⁻² in PC₂₀). However, similar to the RDE experiments, there is no statistical difference between j_{max} obtained using PC₁₂, PC₁₄ or PC₁₆, while the apparent O_2 concentration is increased in the presence of either PC₁₈ or PC₂₀ ($j_{max} = 0.94 \pm 0.14$ mA cm⁻² and $j_{max} = 1.14 \pm 0.15$ mA cm⁻², respectively). A more thorough analysis of CV results and experimental procedures is provided in the ESI† (Fig. S3–S5).

In order to provide a distinction between O_2 transport and localized O_2 concentration, j_{max} was measured under both stirred and quiescent conditions. The resulting CVs reveal that,

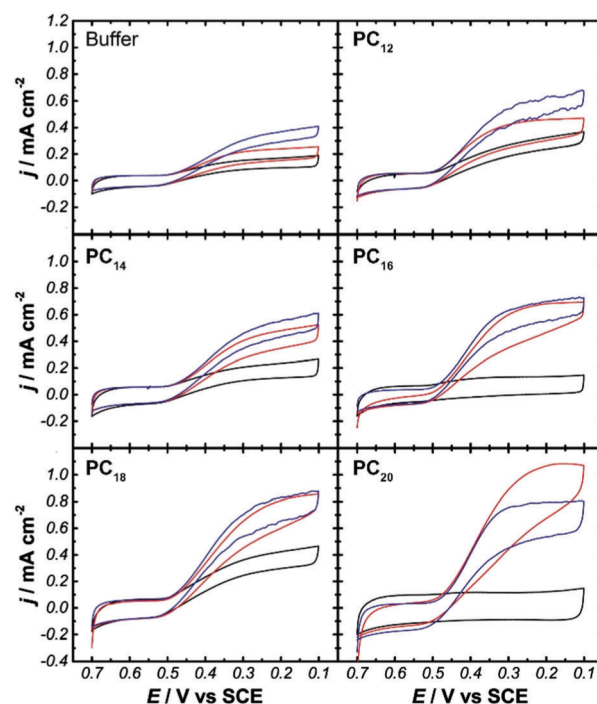


Fig. 2 Representative CVs of BOx biocathodes under N_2 saturation (—), quiescent O_2 saturation (—) or stirred O_2 saturation (—) in solutions containing buffer alone or with 0.5 mM PC₁₂, PC₁₄, PC₁₆, PC₁₈ or PC₂₀. Experiments were performed at 5 mV s⁻¹ using 200 mM citrate/phosphate buffer, pH 6.5, at 25 °C.



as expected, j_{\max} increases with stirring for **PC**_{12–18}; this reflects increased O₂ transport to the electrode surface. However, the difference in stirred vs. quiescent j_{\max} decreases as PC chain length increases to the extent that stirring lowers j_{\max} in solutions of **PC**₂₀. While the precise nature of this result is unclear, it indicates that the phospholipids are allowing for increased local O₂ concentration at the surface of the electrode as opposed to increasing O₂ concentration throughout the bulk solution.

We next aimed to determine the duration of these unexpected effects. To accomplish this, O₂ retention times at BOx biocathodes were measured amperometrically as above using stirred solutions containing PCs of various length (Fig. 3). The resulting $t_{1/2}$ values demonstrate a similar correlation between state of phase and retention time that was observed at Pt RDEs. However, O₂ retention time measured by BOx biocathodes was greater than 10 times longer for solutions of **PC**₂₀ (1800 ± 200 s) than for buffer (270 ± 100 s). Additionally, the increase in $t_{1/2}$ for all studied PCs beyond the control buffer was significantly greater when studied at the BOx biocathodes than the Pt RDE, suggesting a fundamental difference in the mechanism of O₂ transport between the biocathode and Pt electrode interface.

Based on the large discrepancy in $t_{1/2}$ between electrode materials, we turned our attention towards methods to study the BOx biocathode surface in the presence of PCs. Unfortunately, fluorescence images of BOx-modified Toray paper electrodes revealed a strong background fluorescence from the anthracene-modified CNTs used to prepare the electrode material. Consequently, a (7-nitro-2-1,3-benzoxadiazol-4-yl)amino (NBD)-modified **PC**₁₈ was used as a fluorescent probe to compare the behavior of PCs in solution with that at the surface of an unmodified Toray electrode. Fluorescence images of NBD-**PC**₁₈ (provided in the ESI,† Fig. S9–S28) indicate that solid-phase lipids in solution are distributed homogeneously, while similar images of NBD-**PC**₁₈ in the presence of a Toray paper electrode reveal the formation of phospholipid aggregates on the electrode surface. Taken together with the observed increase in catalytic current density of BOx biocathodes in quiescent solutions,

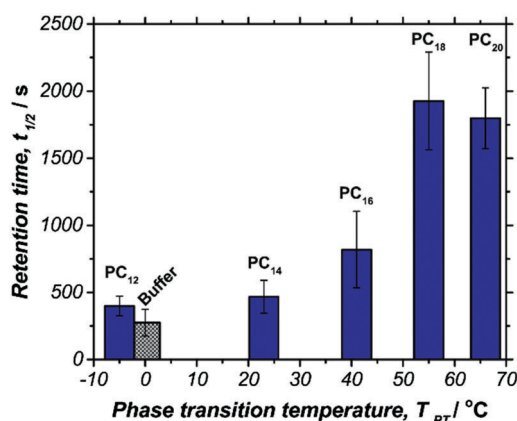


Fig. 3 PC phase transition temperature versus retention time ($t_{1/2}$) for solutions containing 0.5 mM PC. Retention time was measured amperometrically by 1 cm² BOx biocathodes using 200 mM citrate/phosphate buffer at pH 6.5 and 25 °C.

this suggests that **PC**₁₈ and **PC**₂₀ aggregates are trapping O₂ at the biocathode surface, allowing for enhanced localized O₂ concentration. (Full fluorescence analysis of phospholipid interactions at the biocathode surface are provided in the ESI†).

Having established the use of **PC**₂₀ to enhance the apparent O₂ concentration at a BOx biocathode surface, the next step was to determine its compatibility in a fully enzymatic biofuel cell. We employed a recently reported glucose bioanode that uses a naphthoquinone-modified linear poly(ethylenimine) (NQ-LPEI) hydrogel to immobilize flavin adenine dinucleotide-dependent glucose dehydrogenase (FAD-GDH).⁴ This material utilizes naphthoquinone as a low-potential electron mediator to allow for increased cell potential, while the FAD-GDH does not use O₂ as a natural electron acceptor and as such, mediated enzymatic glucose oxidation does not compete with enzymatic O₂ reduction.

EFCs were constructed to have a bioanode and biocathode of equal surface area (1 cm × 1 cm Toray electrodes) and were characterized by linear polarization at 1 mV s⁻¹ using solutions of 100 mM glucose. Power and current density curves of EFCs tested using quiescent solutions in the presence and absence of 1 mM **PC**₂₀ are presented in Fig. 4. EFCs performed using

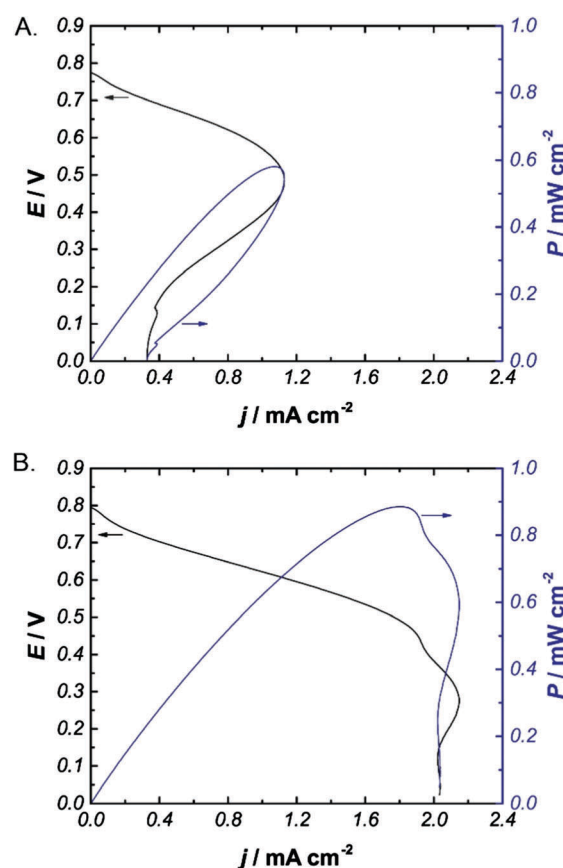


Fig. 4 Representative power and current density curves for EFCs in a quiescent solution without (A) or with (B) 1 mM **PC**₂₀. EFCs were constructed with naphthoquinone-modified LPEI (NQ-LPEI)/FAD-GDH bioanodes and anthracene-modified carbon nanotubes (An-CNTs)/BOx using solutions of 200 mM citrate phosphate buffer, pH 6.5, with 100 mM glucose at 25 °C.



solutions with 1 mM PC₂₀ exhibited a 10-fold increase in current density (j_{\max}) and power density (P_{\max}) compared to those tested in quiescent solutions containing glucose alone ($j_{\max} = 1.9 \pm 0.4 \text{ mA cm}^{-2}$ and $P_{\max} = 0.8 \pm 0.2 \text{ mW cm}^{-2}$ versus $j_{\max} = 0.100 \pm 0.009 \text{ mA cm}^{-2}$ and $P_{\max} = 0.061 \pm 0.005 \text{ mW cm}^{-2}$). Comparison of the corresponding power curves indicates that the majority of the increase in current density occurs at low resistance in the diffusion-limited region of the curve. Combined with control experiments (provided in the ESI†) demonstrating a high limiting anodic current density ($j_{\max} = 2.2 \text{ mA cm}^{-2}$), these results suggest that the increased j_{\max} and P_{\max} are a result of increased O₂ concentration at the biocathode.

In conclusion, we have identified a series of commercially available phospholipids capable of trapping O₂ in an aqueous solution and increasing its residence time at the surface of a biocathode. Additionally, the solid-phase phosphocholine, PC₂₀, was used to increase the local apparent O₂ concentration at the surface of a BOx-modified biocathode, resulting in a catalytic current density of $1.1 \pm 0.1 \text{ mA cm}^{-2}$ for ORR at 25 °C and physiological pH. While this methodology was described in the context of EFCs, it has a direct potential application in *ex vivo* microbial fuel cells. Furthermore, we believe that this work will provide a foundation for engineering solutions to address the problem of aqueous O₂ transport. Finally, PC₂₀ was demonstrated as a simple EFC additive to enhance current and power outputs without the need for artificial convection.

The authors would like to thank the National Science Foundation, Air Force Office of Scientific Research, and the Army Research Office for funding. The authors would also like to thank Matt Judge and Derek Jensen for collecting the EFC data.

Notes and references

- 1 W. Schuhmann, T. J. Ohara, H. L. Schmidt and A. Heller, *J. Am. Chem. Soc.*, 1991, **113**, 1394–1397.
- 2 M. T. Meredith, D.-Y. Kao, D. Hickey, D. W. Schmidtke and D. T. Glatzhofer, *J. Electrochem. Soc.*, 2011, **158**, B166–B174.
- 3 B. Reuillard, A. Le Goff, C. Agnes, M. Holzinger, A. Zebda, C. Gondran, K. Elouarzaki and S. Cosnier, *Phys. Chem. Chem. Phys.*, 2013, **15**, 4892–4896.
- 4 R. D. Milton, D. P. Hickey, S. Abdellaoui, K. Lim, F. Wu, B. Tan and S. D. Minter, *Chem. Sci.*, 2015, **6**, 4867–4875.
- 5 S. Tsujimura, Y. Kamitaka and K. Kano, *Fuel Cells*, 2007, **7**, 463–469.
- 6 K. MacVittie, T. Conlon and E. Katz, *Bioelectrochemistry*, 2015, **106**(Part A), 28–33.
- 7 R. Battino, T. R. Rettich and T. Tominaga, *J. Phys. Chem. Ref. Data*, 1983, **12**, 163–178.
- 8 E. P. Wesseler, R. Iltis and L. C. Clark Jr, *J. Fluorine Chem.*, 1977, **9**, 137–146.
- 9 E. Katz, B. Filanovsky and I. Willner, *New J. Chem.*, 1999, **23**, 481–487.
- 10 S. Reiter, K. Habermüller and W. Schuhmann, *Sens. Actuators, B*, 2001, **79**, 150–156.
- 11 S. C. Barton, H.-H. Kim, G. Binyamin, Y. Zhang and A. Heller, *J. Phys. Chem. B*, 2001, **105**, 11917–11921.
- 12 L. Stoica, N. Dimcheva, Y. Ackermann, K. Karnicka, D. A. Guschin, P. J. Kulesza, J. Rogalski, D. Haltrich, R. Ludwig, L. Gorton and W. Schuhmann, *Fuel Cells*, 2009, **9**, 53–62.
- 13 M. Falk, Z. Blum and S. Shleev, *Electrochim. Acta*, 2012, **82**, 191–202.
- 14 K. Stolarczyk, E. Nazaruk, J. Rogalski and R. Bilewicz, *Electrochim. Acta*, 2008, **53**, 3983–3990.
- 15 G. Gupta, V. Rajendran and P. Atanassov, *Electroanalysis*, 2004, **16**, 1182–1185.
- 16 S. Calabrese Barton, *Electrochim. Acta*, 2005, **50**, 2145–2153.
- 17 M. G. Scott, D. F. Kucik, L. T. Goodnough and T. G. Monk, *Clin. Chem.*, 1997, **43**, 1724–1731.
- 18 J. S. Jahr, S. B. Nesargi, K. Lewis and C. Johnson, *Am. J. Ther.*, 2002, **9**, 437–443.
- 19 J. N. Kheir, L. A. Scharp, M. A. Borden, E. J. Swanson, A. Loxley, J. H. Reese, K. J. Black, L. A. Velazquez, L. M. Thomson, B. K. Walsh, K. E. Mullen, D. A. Graham, M. W. Lawlor, C. Brugnara, D. C. Bell and F. X. McGowan, *Sci. Transl. Med.*, 2012, **4**, 140ra188.
- 20 B. Olmeda, L. Villén, A. Cruz, G. Orellana and J. Perez-Gil, *Biochim. Biophys. Acta, Biomembr.*, 2010, **1798**, 1281–1284.
- 21 M. T. Meredith, M. Minson, D. Hickey, K. Artyushkova, D. T. Glatzhofer and S. D. Minter, *ACS Catal.*, 2011, **1**, 1683–1690.

